Population changes and sustainability of energy drive cooling demand related risks in urbanized India

Abstract

Global warming poses a challenge to India's energy policy as rising temperatures coincide with population growth and lifestyle changes to substantial increase in cooling energy requirements. The concept of cooling degree-days (CDD) is often used to assess probable changes in cooling demands but, to date, no study has considered CDD changes within a risk framework to consider exposure and underlying vulnerabilities of a population. Here, we quantify the trends in observed CDD data across administrative divisions of India for 1951-2019. Using temperature data from five climate models under three representative concentration pathways (RCPs), we then estimate the relative changes in average annual CDD across India under 1.5°C, 2°C and 3°C levels of global warming. We further quantify the risk associated with increased cooling requirements for most urbanized regions of India using CDD as hazard, population as exposure, and two alternative vulnerability metrics that account for economic conditions (per capita Gross Domestic Product, GDP) and energy source (proportion of renewable energy to total energy). For 62% of administrative units, the Pettitt's test identified a statistically significant change point in annual CDD values, with 1993 as the median year of change. Climate model projections suggest a likely increase of 5-14%, 13-80% and 22-160% in average annual CDD values for a majority (>90%) of administrative units under the 1.5°C, 2°C and 3°C levels of global warming, respectively. The risk assessment showed that population exposure was the primary factor governing risk scores when per capita GDP was used as a proxy for vulnerability. Risk scores differed substantially when the vulnerability index was based on contribution of non-renewables to electricity requirements. Our analysis emphasizes

that prevailing socio-economic conditions and energy policies are likely to play a strong role in mitigating climate change impacts related to cooling energy requirements in urbanized Indian regions.

Keywords: Cooling Demands, Global Warming, Risk Assessment, Cooling Degree Days, Urban, India, Population Growth, Renewable Energy, Electricity, Carbon Emissions

1. Introduction

Global warming has become a major environmental concern in the last few decades, with global mean surface temperature rising by 0.87°C in 2006-2015 relative to 1850-1900 (Hoegh-Guldberg et al. 2018). Increasing global temperatures have coincided with an increase in frequency of heatwaves in most land as well as marine regions (Baldwain et al. 2019; Frölicher et al. 2018). Due to the intensification of the hydrological cycle, the frequency of floods and droughts have also increased at the global scale (Zhang et al. 2019). These changes threaten many natural ecosystems as well as agri-ecosystems by impacting crop yields (Hoegh-Guldberg et al. 2018). In addition, fisheries and aquaculture also face increasing risk from ocean warming and acidification (Reverter et al. 2020).

As of 2012, India contributed 5.7% of global carbon emissions of 34.5 billion tons/year maintaining a per capita emission of 1.6 tons/ person (Olivier et al. 2013). India aims to reduce its carbon emissions intensity (CO_2 emissions per GDP) by 33-35% by 2030 from 2005 levels, which will be enabled, in part, by a transition to cleaner energy sources as India aims to generate 40% of the electricity from non-fossil sources (Zhu et al. 2018). Nearly a third of the electricity generated in India is consumed by domestic and commercial sectors, which includes household and commercial cooling demands. The contribution of cooling requirements to electricity consumption is poised to increase sharply in the coming years as a result of increasing appliance ownership (IEA, 2021). For example, Indians may operate nearly 1 billion air conditioning units by 2050. According to the latest assessment by IEA (2021), under a standard policy scenario, the electricity demand for cooling may increase by six-fold by 2040, with electricity use peaking in early evening. At present, nearly 80% of electricity requirements are met by thermal power plants while remaining from nuclear (~2%), hydro-electricity (8.7%), and other renewable sources (8.3%) (MoSPI, 2020). Energy access is still poor and unreliable, in fact, energy poverty is more prevalent as compared to income poverty in India (MoSPI, 2020; Sedai et al., 2020). Thus, the energy policy for India needs to address the challenges of sustainability and equity in distribution of energy while also reducing carbon emissions (Solanki et al., 2020).

Global warming related heatwaves will result in increasing energy requirements and cause power outages due to unprecedented peaks in electricity use (Ciancio et al. 2020; Zhang et al. 2021; Petri and Caldeira 2015; Mishra et al., 2019; Lipson et al., 2019 and Yaduvanshi et al., 2021). Thus, innovative strategies for building cooling requirements need to be developed that can be either applied during construction or retrofitting stages (Ascione et al. 2017; Balaban and de Oliveira, 2017; Zhao et al. 2019; Hossain and Poon, 2018; Zhang et al. 2021). These approaches include novel cooling systems design such as the roof-integrated radiative air-cooling system proposed by Zhao et al. (2019), adopting solar absorption air-conditioning (Solano-Olivares, 2019), etc. Long-term energy planning of buildings using a multi-stage multi-objective approach to identify the suite of best possible energy conservation measures would also enable a transition to sustainable building designs (Ascione et al. 2017). As the extensive use of air conditioning is also likely to have a detrimental impact through the urban heat island effect, design of sustainable air conditioning systems would be crucial in mitigating negative health impacts of global warming (Tremec et al. 2012).

In order to design and manage buildings under warming conditions, planners require information regarding the probable changes in cooling requirements in the future. Air temperature followed by relative humidity are the dominant climatic variables affecting energy consumption in a building (Sailor et al., 2011; Lee et al., 2014; Kumar et al., 2020; Maia-Silva et al., 2020). The concept of degree days is often used to relate outside climatic conditions and energy consumption (Thom, 1959; Quayle and Diaz, 1980, De Rosa et al., 2014). Two related variables: heating degree days (HDDs) and cooling degree days (CDDs), are commonly used to calculate the energy required to warm up and cool down buildings, respectively. Although the use of degree-days has some shortcomings (Mc Intyre *et al.,* 1987; Moral-Carcedo and Vicens-Otero, 2005; Antunes Azevedo *et al.,* 2015), they are widely applied for climatological and impact analysis in India (Gupta et al., 2012, Borah et al., 2014; Bhatnagar et al., 2018) as well as other regions (e.g., Wang *et al.,* 2010; Castañeda and Claus, 2013; Spinoni et al., 2018, Morakinyo et al., 2019; Shi et al., 2018; Ramon et al., 2020; Islam et al., 2020).

A number of studies have assessed the historical changes in CDD values at various spatial scales such as cities (Badescu et al., 1999), countries (Morakinyo et al., 2019; Islam et al., 2020) and buildings (Christenson et al., 2006; Bhatnagar et al., 2018). More recently, Biardeau et al. (2020) estimated global air conditioning requirements based on CDD values using population and daily temperature data across 1692 cities in the world. They reported that India has highest exposure to rising CDD compared to any other place in world. The application of degree days indicators in energy studies on India has been spatially restricted to buildings, cities, or specific regions as well as temporarily to short historical periods at hourly or daily scale (Shanmugapriya et al., 2011; Borah et al., 2015; Bhatnagar et al., 2018). For example, Borah et al. (2015) analysed HDD and CDD for three climatic zones in northeast India and found that hourly temperature data is more suitable than daily data for degree days calculation. However, availability of hourly temperature data can be challenging. Desai et al. (2019) have developed a python-based toolbox to estimate energy consumption for 59 Indian cities covering five types of buildings using hourly temperature data.

In our study, we make two main contributions. First, we analyse the spatiotemporal trends in CDD across India at the scale of fine administrative units for the historical time period using observational datasets. To date, a country-wide assessment of CDDs has not been carried out using available observations, and our analysis would help understand the changes in cooling requirements in recent past. Our second contribution is the development of a framework that quantifies the risk associated with rising CDDs in the future using downscaled climate model outputs and two different vulnerability indicators. We use per capita Gross Domestic Product (GDP) to represent the ability to cope with rising energy demands. We also include a sustainability oriented vulnerability metric that quantifies the relative contribution of non-renewable energy to total energy usage in electricity. In addition, our risk framework quantifies future exposure using projected population under different Shared Socioeconomic Pathways (SSPs; Riahi et al., 2017). Specifically, we address the following objectives:

1. Analyse the spatiotemporal changes in CDD values in the historical time period (1951-2019) across India.

2. Quantify the projected changes in CDD values under 1.5°C, 2.0°C, and 3.0°C warming worlds and associated uncertainties.

3. Quantify the risk of CDD exposure in ten most urbanized regions in India and understand how risk is related to CDD and other factors.

2. Data and Methods

2.1 Data

We performed our analysis for lower-level administrative divisions of India, termed districts. The choice of the spatial scale is made considering that districts are often considered as a unit for program implementation and development planning in India. The data sources used in the study are summarized in Table 1. As the temperature data is available as a gridded product, it is area-averaged to obtain district-wise estimates. Observed temperature data from 1951-2019 is used to analyse the statistical trends in CDD. Observed population data for the year 2011 can be downloaded from https://www.census2011.co.in/city.php. GDP data for 2011 is available at https://www.aegonlife.com/insurance-investment-knowledge/which-are-indias-top-10-cities-by-gdp/.

Future projections of temperature are obtained from the downscaled and bias-corrected product developed under the Inter-Sectoral Impact Model Intercomparison Project (ISI-MIP, Warszawski et al., 2014). The projections are available for five general circulation models (GCMs) from the coupled model intercomparison project-5. These are: GFDL–ESM2M, HadGEM2–ES, IPSL–CM5A–LR, MIROC–ESM–CHEM, and NorESM1–M. Projections are available for three representative concentration pathways (RCPs), RCP2.6, RCP6.0 and RCP8.5. Population and GDP projections are obtained at 0.5° grids for decadal time steps from 1980 to 2100 (Murakami and Yamagata, 2019; http://www.cger.nies.go.jp/gcp/population-and-gdp.html). This global dataset was generated by downscaling the urban population, nonurban population, and gross domestic productivity (GDP) (Billion USD at 2005-year rate) by country under three shared socioeconomic pathways (SSPs) namely, sustainability (SSP1), middle of road (SSP2) and regional rivalry (SSP3). SSPs are generated by considering various aspects such as climate change vulnerability, adaptation, land use change, and emission pathways that wield control over demography (O'Neill et al., 2014). Projections of population and GDP for each district for 1.5°C, 2.0°C, and 3.0°C WLs are estimated as the median value out of decadal SSPs datasets, following procedures described in Singh and Kumar (2019) and Kumar and Mishra (2020). The projected population and GDP are used to estimate relative change values between future and reference periods and are applied to the year 2011 values.

Table 1. Various data products used in the analysis along with their spatial resolution, time period and associated data sources.

SNo.	Variable	Spatial Resolution	Time Period	Data Source	Reference
1	Observed Daily Mean Temperature	1°x1°	1951-2019	India Meteorological Department, IMD	Gupta et al., 2020
2	Projected Daily Mean Temperature	0.5°x0.5°	2005-2100	Inter-Sectoral Impact Model Intercomparison Project ISI-MIP	Warszawski et al., 2014
3	Observed Population Data	District	2011	Census-2011	Singh and Kumar, 2019
4	Projected Population Data	0.5°x0.5°	1980-2100	SSP 1 to SSP 3	Murakami and Yamagata, 2019
5	Observed GDP	District	2011		Business World-June 2017
6	Projected GDP Data	0.5°x0.5°	1980-2100	SSP1 to SSP3	Murakami and Yamagata, 2019
7	Relative contribution of non-renewables to electricity suppplied	District	2020	Carbon Disclosure Project (CDP Portal)	CDP-ICELI Unified Reporting System

2.2 Estimation of Cooling Degree Days (CDDs) and Statistical Analysis

Degree days are a climate statistic originally developed by the US utility companies in the 1930s for estimating the demand for coal and gas based upon typical energy usage (Sailor and Munoz, 1997; Borah et al., 2015). CDD is estimated as an accumulated difference between the daily mean temperature and a given reference temperature over a certain period (Barger and De, 2001). We calculate CDDs values using Eq. (1).

$$CDD = \sum_{t=1}^{n}(T_d(t) - T_b) \quad for\ T_d(t) \geq T_b;\ else\ 0. \qquad (1)$$

In Eq. (1), temperature T_d(t) is the daily mean temperature [°C], T_b is the reference temperature [°C], t is the index for each day from the first to nth day in a year. It follows that the units of CDD is also °C. The CDD value thus obtained is for each year by adding daily values. The CDD value for a time period spanning several years is obtained by averaging the annual CDD values across all years.

The reference temperature should be chosen such that it adequately represents the threshold beyond which cooling requirements emerge in a given climate. It therefore incorporates the effects of local conditions on cooling requirements. Thom (1952) first adopted a value of 18.3°C, which was also used by the recent global analysis by Biardeau et al. (2020). Several choices have been used in the past such as 18°C, 20°C, 26°C and 28°C (Kadioglu and Sen 1999; Yildiz and Sosaoglu 2007; Elizbarashvilli et al. 2018). For India, Bhatnagar et al. (2018) identified 18°C as the reference temperature for cooling and heating after performing an energy simulation-based analysis for 60 cities of India. Here, we have also adopted 18°C as the reference temperature following the India-wide analysis by Bhatnagar et al. (2018).

Two statistical tests, namely the Pettitt's test and the Mann-Kendall's test (Kendall, 1975), are applied on annual CDD time series to assess whether any break or trends are present in annual CDD values. We first apply the Pettitt's test to identify change points in the data. Then the Mann-Kendall's test is used to identify significant monotonic changes in annual CDD values after the change point to focus on recent trends in annual CDD values. The Pettitt's test is one of the important non-parametric tests to assess the change in a time series (Pettitt, 1979; Sneyers, 1991; Verstraeten et al. 2006). According to Pettitt's test, x_1, x_2,…, x_n is a series of observed data with a change point at time t such that the distribution of data points prior and after the point t is $F_1(x)$ and $F_2(x)$, respectively. The non-parametric test statistics U_t for this test is estimated using Eq. (2). The test statistic K and the associated confidence level (ρ) for the sample length (n) are estimated using Eqs. (3-4).

$$U_t = \sum_{i=1}^{t} \sum_{j=t+1}^{n} sign\ (x_t - x_i) \quad (2)$$

$$K = Max\ |U_t| \quad (3)$$

$$\rho = \exp\left(\frac{-K}{n^2 + n^3}\right) \quad (4)$$

The series will be divided into two parts at the location of change point where the significant change point exists. If the p-value is less than the significance level α, the null hypothesis that no change in the distribution of a sequence of random variable is considered to be rejected. Further details on the Pettitt test can be found in Jaiswal et al. (2015) and Dhorde and Zarenistanak (2013).

The Mann-Kendall trend test is widely used in detecting statistically significant tendencies in environmental datasets, and has been recommended by the World Meteorological Organization (Irannezhad et al. 2014; Gavrilov et al. 2016). The test is based on a null hypothesis (H0) that states that there is no trend in the time series and the data are independent and randomly ordered. The alternative hypothesis (Ha) indicates a trend in the time series. The test statistic S for a time-series (x) is estimated using Eq. (5).

$$S = \sum_{i=1}^{n-1} \sum_{j=i+1}^{n} sgn\ (x_j - x_i) \quad (5)$$

In Eq. (5), *sgn* represents the signum function. Hence a large positive value indicates that the later observations are larger than the previous ones, thereby indicating a positive trend, and vice versa. An advantage of this test is that the assumption of normality is not required (Helsel and Frans 2006).

2.3 Risk assessment framework

Global warming coupled with increasing population, income and urbanization are likely to contribute to a steep rise in cooling demands (Campbell et al., 2018 and Khosla et al., 2021). India has about four times more population and three times as many CDDs per person as the United States (Sivak et al., 2013). Most analyses of cooling risk using CDD focus on the hazard, i.e., changes in CDD and its trends. However, the severity of risk associated with increasing CDD values would be modulated by exposure of the population as well as underlying vulnerabilities. Climate-related risk analyses on hazards such as heat waves (He et al., 2019 and Estoque et al., 2020), floods (Canccado et al., 2008; Kazmierczak and Cavan, 2011 and Armenakis et al., 2017), and droughts (Cardona 2011 and Prabnakorn et al.,2019) conceptualize risk as a function of hazard, exposure and vulnerability, a definition also adopted by the Fifth Assessment Report of the Intergovernmental Panel on Climate Change (IPCC, 2014). This framework is in line with the field of disaster risk reduction and Crichton's risk triangle (UNSIDR, 2017; Crichton, 1999).

Following prior approaches, we define risk considering the three dimensions of hazard, exposure, and vulnerability. *Hazard* is a natural phenomenon that may cause damage to people, property, and the environment. *Exposure* is defined as the extent with which an environmental hazard affects a group of people or the system. *Vulnerability* captures the susceptibility of the exposed system or people to damage. Vulnerability is characterized by the physical, social, and economic conditions of the system that make it susceptible to the damaging effects of a hazard (Philip and Rayhan, 2004). It is possible to be exposed but not vulnerable. For instance, people residing in heat wave affected areas could cope up with hazard depending on the availability of sufficient (cooling) means. The risk associated with hazard, exposure and vulnerability metrics can be combined using Eq. (6) (INFROM Global Risk Index, 2018; Cardoni et al., 2021). In Eq. (6), the hazard is quantified using average annual CDD values across the time period of assessment, and exposure is quantified as the population of the region for which CDD is assessed.

$$Risk = (Hazard * Exposure * Vulnerability)^{\frac{1}{3}} \tag{6}$$

Vulnerability is a critical factor in risk calculations and also one that is more difficult to quantitatively characterize. Here, we considered two aspects related to rising degree-days that may affect populations in the context of cooling energy requirements: 1) the economic resource available to a population to respond to rising cooling demands, and 2) the relative amount of cooling energy being supplied by non-renewable sources as compared to the renewable sources. Per capita GDP has often been used to characterize a population's ability to cope with heat stress (Jagarnath et al., 2020), and therefore used here similarly. Higher values of per capita GDP will be associated with lower risk scores as populations with elevated income levels would have adequate means to deal with higher temperatures (Bosello et al., 2006, Ahmadalipour et al., 2019). The source of energy becomes crucial from a sustainability perspective. Regions heavily dependent on non-renewables witnessing increasing degree-days are likely to pose a greater risk from increasing carbon emissions. Note also that data limitations prohibited a detailed exploration of implications of energy sources. So, the comparison across vulnerability metrics is limited to five urbanized districts while per capita GDP based risk metrics are compared across ten urbanized districts.

Each component is re-scaled to vary from 1 to 10 so that none of the individual components dominate the risk calculation (Eq. 7, INFROM Global Risk Index, 2018). In Eq. (7), X_{scaled} is the scaled value of the variable, X_{es} is estimated value of variable (hazard, exposure and vulnerability) at a given location, X_{min} and X_{max} are the minimum and maximum value of the variable across all locations and warming levels. Per capita GDP values are multiplied by -1 prior to scaling as it is inversely related to risk score.

$$X_{scaled} = 1 + 9\left(\frac{X_{es} - X_{min}}{X_{max} - X_{min}}\right) \tag{7}$$

2.4 Projections at different warming levels

A warming level corresponds to a time period when the global mean temperature rises above the pre-industrial level by the amount specified by it. Each GCM-RCP combination will reach a certain warming level in a different time period as it represents varying climate dynamics and forcings. These time periods are identified using the approach proposed by Vautard et al. (2014), which has been used in a number of recent analyses (Masson-Delmotte et al. 2018, Singh and Kumar 2019; Kumar and Mishra, 2020; Sieck et al., 2021). Historical records indicate that the global mean temperature for the reference period 1971-2000 was around 0.46°C higher than the pre-industrial period (1881-1910) (Jacob et al., 2018). Thus, the procedure identifies 30-year time periods when global mean temperature reaches 1.04°C, 1.54°C and 2.54°C above the reference period (Supplementary Table S1). Then, the relative change in average annual CDD for each GCM-RCP combination is calculated by using the average annual CDD values for the reference period 1971-2000 as a baseline using Eq. (8).

$$R = 100\left(\frac{(CDD_F+1)-(CDD_R+1)}{CDD_R+1}\right) \tag{8}$$

In Eq. (8) R is the relative change in %, CDD_R and CDD_F are the average annual CDD values for the reference period and future period, respectively. Note that both values are incremented by 1 to allow finite values of R in cases when reference period value may be 0. Using three RCPs and five GCMs results in 15 GCM-RCP combinations for which relative change in CDD is projected for each warming level. The risk analysis uses median values of average annual CDD across the 15 GCM-RCP.

3. Results and Discussion

We begin our results section with a description of observed trends in CDD for the historical time period 1951-2019 (Section 3.1). Following this, the projected changes in CDD across India are discussed for each warming level (Section 3.2). We conclude with the risk analysis for most urbanized regions is detailed in Section 3.3.

3.1 Spatiotemporal trends in observed CDD for 1951-2019

Mean annual CDD values for 1951-2019, as estimated by observed IMD data, range from 586°C to 3863°C across the districts of India (Figure 1a). As expected, the lowest mean annual values of CDD are found northern most regions of the country that are dominated by mountainous terrains and cooler climate. Notably, highest CDD values (>3000°C) are found in the eastern parts of Peninsular India, despite the presence of the Thar desert in the north-western region. Despite recording highest daily temperatures during summers, the CDD values in these drier (desert) dominated districts remain lower than the regions in eastern Peninsular India because of lower winter temperature. We also find a distinct rise in annual CDD values in the recent years (Figure 1b). The mean annual CDD value has been exceeding 4000°C in a few districts since 1980.

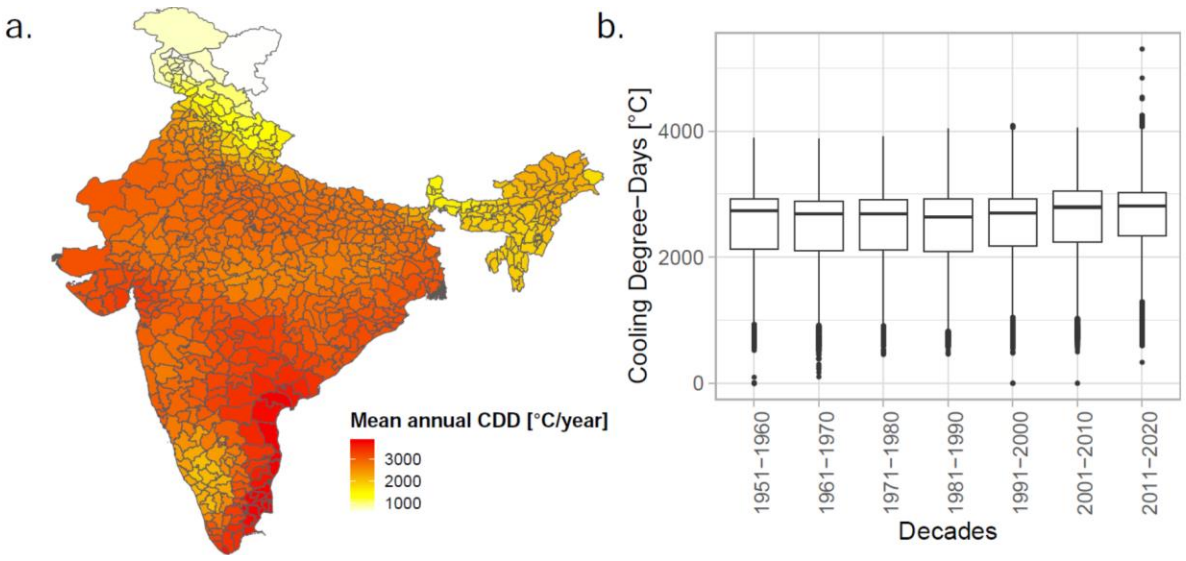

Figure 1. (a) Spatial distribution of observed mean annual cooling degree-days (CDD) values [in °C] across India for 1951-2019. (b) Boxplot of observed annual CDD (x-axis) across all administrative units for each decade. The median CDD value for each decade is represented by the horizontal black line within the box while the edges represent the 25th and 75th percentile CDD values. The whiskers extend from the box to 1.5 time the inter-quartile range, the difference of 75th and 25th quartiles. Data beyond range of whiskers are shown individually.(Coloured Figure)

The Pettitt's test identified a large range (1961-2008) of change points in annual CDD time series across India for 1951-2019 (Figure 2a). However, only 62% of these change points were statistically significant with p-Value < 0.01. The median value of the year of abrupt change in annual CDD for statistically significant change points was 1993, while the 25th and 75th quantile of change years was 1981 and 1997, respectively. The year of abrupt change in annual CDD occurred earliest in south eastern India around 1970, followed by the southern peninsular region around 1980. For regions with statistically significant change points, we further carried out the Mann-Kendall test on the annual CDD times series after the change point (Figure 2b). The Sen's slope ranged from 2.93 to 16.87 °C/year for regions with statistically significant (p-Value

< 0.01) trends. Highest slopes are observed for the mountainous regions in northeast India although the change point there occurred later. Note also that the Mann-Kendall test identified an increasing trend for a majority (88%) of regions in India after the change point, even though many of these were not statistically significant.

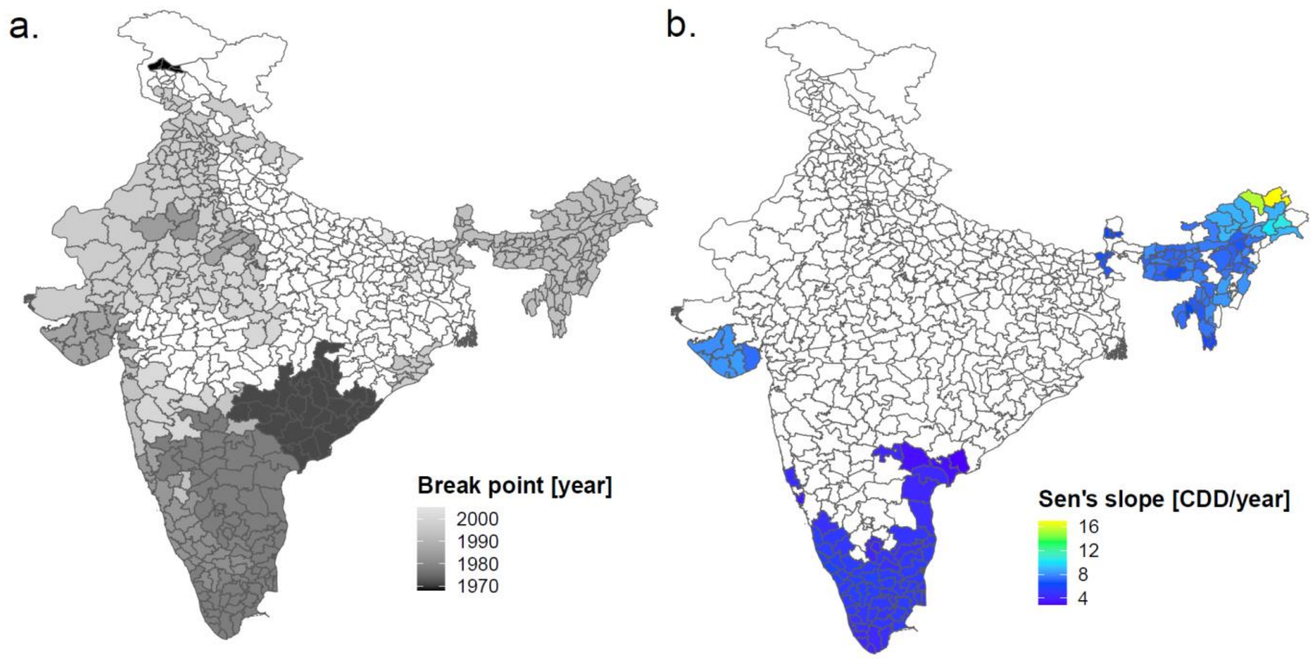

Figure 2. a) The year of abrupt change in annual CDD values as identified by the Pettit's test for each administrative unit 1951-2019. Only statistically significant (p-Value < 0.01) change points are shown in grey scale and further analysed by the Mann-Kendall test. b) Sen's slope of annual CDD values for administrative units with statistically significant trends as identified by the Mann-Kendall test. The slope is estimated for the time series following the year of abrupt change. In both panels, white regions correspond to p-Value > 0.01 for the Pettitt and Mann-Kendall test. (Coloured Figure)

To further interpret the results from the Pettitt's and Mann-Kendall test, we visualize the observed annual CDD time series for two example regions: Delhi and Chennai (Figure 3). The year of abrupt change in CDD values occurs much later (1997) in Delhi when compared to Chennai (1978). Note also that the change point for Delhi was not statistically significant (p-Value > 0.01). The change in CDD values following the year of abrupt change is also more drastic for Chennai (5.09 °C/year) when compared to Delhi (1.13 °C/year). Again, the trend from Mann-Kendall test is not statistically significant for Delhi, even though it indicates likely increasing CDD values.

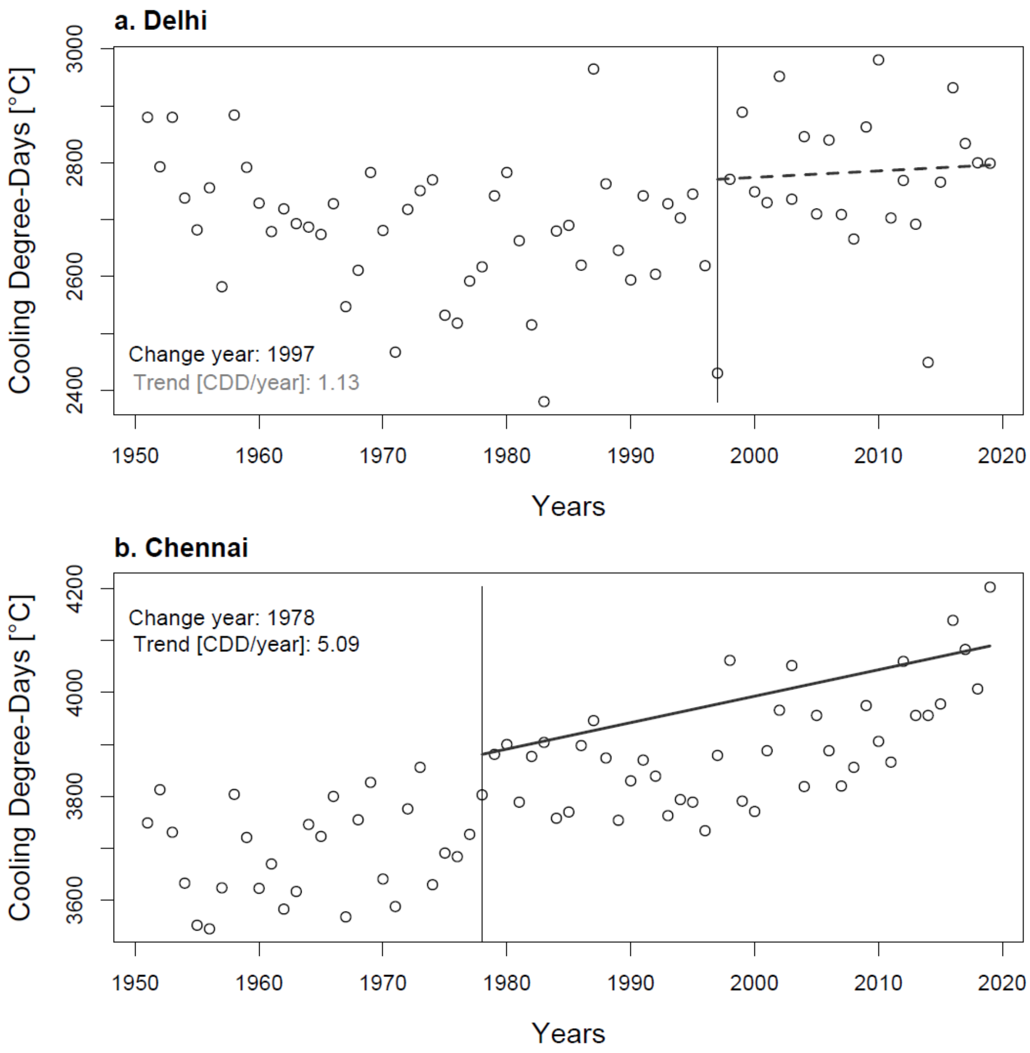

Figure 3. Time series of annual CDD values for a) Delhi, and b) Chennai for 1951-2019. The year of abrupt change in annual CDD values as identified by the Pettit's test is shown as

vertical solid line. Sen's slope for annual CDD values is also shown for the period after the year of abrupt change. Significant trends (p-Value <0.01) as identified by the Mann-Kendall test are highlighted by solid lines for Sen's slope in case of Chennai.

3.2 CDD projections under 1.5°C, 2°C and 3°C warming levels

Cooling demands as represented by CDD values are projected to increase across all regions of India for all three warming levels (Figure 4). The median value of the relative increase in CDD across 15 GCM-RCP combinations is used as an estimate of the likely change in CDD for each warming level and is further analysed. A majority (90%) of regions are likely to experience a 5-14%, 13-80%, and 22-160% increase in average annual CDD at 1.5°C, 2°C and 3°C warming levels, respectively. Note also that as different climate models and concentration pathways attain a warming level at different future periods, these changes are likely to occur between 2006-2076, 2016-2089, and 2035-2096 for the 1.5°C, 2.0°C, and 3.0°C warning levels, respectively (Supplementary Table S1).

The projections show a clear advantage of limiting global warming below 1.5°C, when compared to 2.0°C and 3.0 °C as the former entails much lower average annual CDD values as well as extremes. For example, only 24 regions are likely to experience average annual CDD exceeding 4000°C in the 1.5°C warmer world, but this number rises to 46 (159) in the 2.0°C (3.0°C) warmer world (Figure 4, grey outlines). These extreme CDDs will be experienced first in south-eastern regions that are already known to experience high summer heat. The 3.0°C warmer world presents a concerning picture with large parts of southern peninsula likely to experience average annual CDDs exceeding 4000°C, in addition to regions in the western desert regions and a few along the west coast.

On comparing the performance of GCM projected CDD for the reference period of 1971-2000 to observed data, we find a generally good skill in capturing CDD values across all GCMs (Supplementary Figure S1, Table S2). However, considerable biases are noted for regions with lower CDD values (<2000 °C), especially in northeast India. Climate models used in the present study are known to have cold biases (Basha et al., 2017) especially for Himalayan and North Eastern region (Liu et al., 2014 and Basha et al., 2017). Models that include cloud interaction and aerosols dynamics show relatively less temperature and a cold bias. (Lohmann et al. 2007).

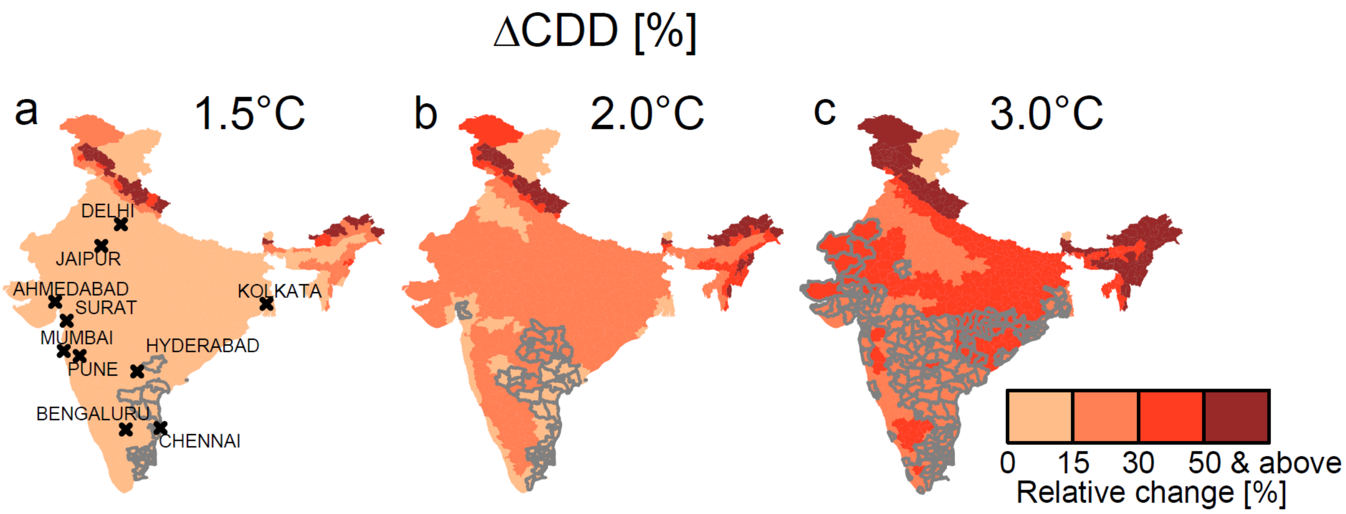

Figure 4. Relative change in average annual CDD values for a) 1.5 °C, b) 2.0 °C, and c) 3.0 °C rise in global mean temperatures compared to pre-industrial levels for administrative units across India. Grey outlines highlight regions with median values of average annual CDD exceeding 4000°C. The median of relative changes values across 15 GCM–RCP combinations is plotted. Panel (a) locates the urban regions considered in the risk analysis. (Coloured Figure)

The future trajectories for annual CDD values exhibit considerable variability across the ten most urbanized regions of India (Figure 5, Supplementary Figure S2). In the reference period, Chennai has the highest average annual CDD values with the median across five climate models as 3945°C. Cooling demands are expected to rise sharply for Chennai under RCP 8.5 when this value is projected to reach 5660°C by the end of the century. Regions such as Surat, Hyderabad, and Ahmedabad are also likely to experience high CDD values (>5500°C) by the end of century under RCP8.5. The maximum average annual CDD values for Delhi, Kolkata, Jaipur, Mumbai and Pune regions are expected to remain below 5000°C, while for Bengaluru and Pune are excepted to remain below 4500°C. The recent analysis by Rai and Ukey (2021) found a similar significant increasing trend in historical and projected CDDs for eight cities across India at decadal scale (1.3-3.8% in 1969-2017). In addition, they also report an expected rise of 8.3%-54.1% in CDD values by 2050 in these cities. These top ten urbanized regions are projected to experience CDD values above the national average under all 15 GCM-RCP combinations, suggesting an increasing demand for household level cooling in urban regions. Elevated levels of CDD coupled with increase in population and GDP could pose a severe challenge on the existing vulnerabilities of urbanised districts, thus necessitating a risk analysis that considers these conditions simultaneously.

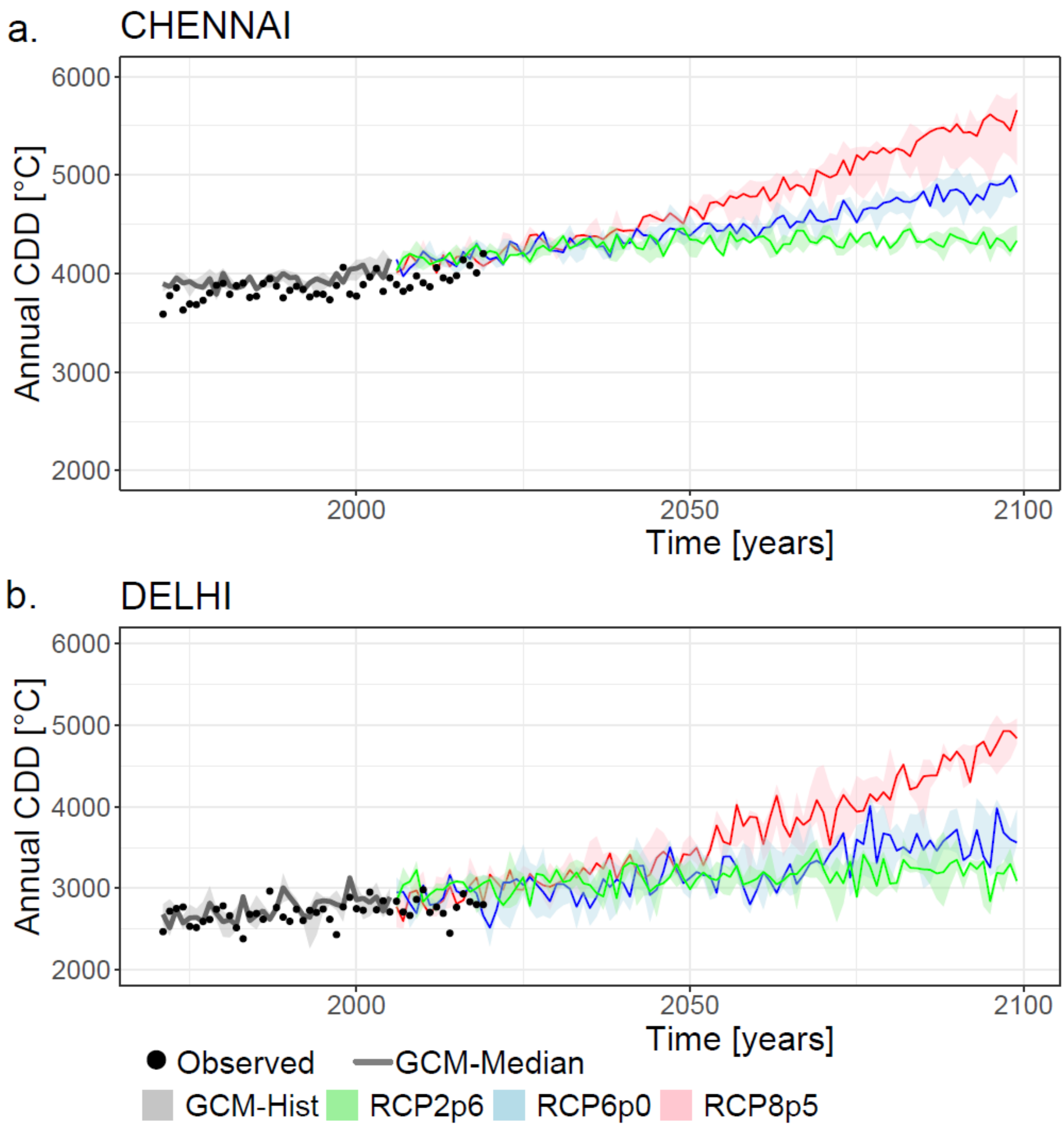

Figure 5. Annual CDD values for a) Chennai and b) Delhi, two of the ten most urbanised districts of India for the time period 1971-2099. Observed CDD is plotted using solid black circles. The ensemble median and inter-quartile range across five GCMs for the period 1971-2005 is indicated by solid grey lines and background grey shades, respectively Coloured lines trace the median CDD across five GCMs for each RCP for the time period 2006-2099. Background shades indicate the interquartile range of annual CDD values across five GCMs. (Coloured Figure)

3.3 Risk assessment for most urbanised districts

The risk associated with CDD hazard was highest for Chennai, Mumbai and Kolkata, in that order, when using GDP per capita as a vulnerability metric and population as exposure metric for the year 2011 (Table 3). These risk scores are primarily driven by population and CDD values, standardized values of these metrics have a Pearson correlation coefficient of 0.65 (p-Value<0.05) with the risk scores. On the other hand, per capita GDP does not play an important role in determining the risk scores for 2011 with Pearson correlation coefficient of -0.1 with risk scores at a p-Value >0.05. While Delhi has greater population, Kolkata's slightly higher CDD value puts it at an overall slightly higher risk on the risk score. Noteworthy is the finding that apart from Chennai and Hyderabad, two other districts with CDD exceeding 3000 degree-days (Ahmedabad and Surat) do not feature in the top 5 most risky districts owing to lower population. Therefore, the risk associated with cooling demands is driven by population followed by CDD values in 2011, with the vulnerability metric (per capita GDP) playing a secondary role.

Table 3: Risk calculation using hazard (CDD), exposure (population) and vulnerability (per capita GDP) for ten most urbanized districts of India for the year 2011.

District	Hazard, CDD [°C]	Exposure, Population [millions]	Vulnerability, GDP per capita [$/person]	Risk Score [-]
Ahmedabad	3276	6.4	10667	4.23
Bengaluru	2409	8.5	10375	2.83
Chennai	3866	8.7	7333	5.56
Delhi	2703	16.3	10438	4.52
Hyderabad	3236	7.7	9250	4.58
Jaipur	2910	3.0	8000	3.08
Kolkata	2986	14.1	10714	4.97
Mumbai	2944	18.4	11611	5.28
Pune	2741	5.0	9600	3.25
Surat	3269	4.6	8000	4.04

Table 4: Risk calculation using hazard (CDD), exposure (population) and vulnerability (per capita GDP) for ten most urbanized districts of India for 1.5°C, 2.0°C, and 3.0°C warming levels.

District	CDD [°C]			Population [millions]			GDP per capita [$/person]			Risk Score [-]		
	1.5°C	2°C	3°C	1.5°C	2°C	3°C	1.5°C	2°C	3°C	1.5°C	2°C	3°C
Ahmedabad	3746	3987	4313	7.2	7.9	8.3	21857	41625	85125	4.81	4.89	4.02
Bengaluru	2933	3157	3484	9.8	11.0	11.4	20100	40455	77636	4.25	4.43	4.00
Chennai	4201	4376	4734	11.1	13.4	15.1	17091	37615	77867	6.10	6.15	5.49
Delhi	2917	3117	3490	18.8	19.3	19.4	20684	42474	81263	5.16	5.16	4.64
Hyderabad	3552	3788	4204	8.7	9.1	9.2	19778	42667	80333	5.01	4.86	4.26
Jaipur	3042	3281	3660	3.3	3.3	3.2	18333	37000	67667	3.15	3.20	3.07
Kolkata	3447	3674	4103	18.0	21.7	24.2	23111	47182	96500	6.00	6.17	4.90
Mumbai	3643	3834	4216	23.7	30.8	37.4	24917	53258	112622	6.86	6.93	4.31
Pune	3055	3262	3657	6.2	7.4	8.3	22000	47714	91000	3.80	3.87	3.38
Surat	3763	3985	4261	5.8	6.8	7.4	18667	41143	98000	4.66	4.70	3.36

On further analysing the risk values under the 1.5°C warming level, we find a similar greater influence of population exposure on the risk scores with a statistically significant high Pearson correlation coefficient between the risk score and standardized population (p-Value < 0.01, coefficient =0.82). Mumbai, with the highest projected population, attained highest risk score despite highest per capita GDP and fourth highest CDD value (Table 4). Neither per capita GDP nor CDD had a statistically significant relationship with the risk scores, but their complementary impact on risk score was evident. For example, even though Chennai ranks 4th in population, it attains the second highest risk score due to highest CDD values and lowest per capita GDP under the 1.5°C warming level.

The impact of rising population on CDD related risk is even more evident in the 2.0°C warmer world with a statistically significant Pearson correlation coefficient between the risk score and standardized population (p-Value < 0.01, coefficient =0.87). In the 2.0°C warmer world, highest risk score is again attained by Mumbai owing to high population and fourth highest CDD. Note that despite having highest per capita GDP, the risk score for Mumbai indicates the possibility of an alarming impact of rising heat related hazard on its population. Similarly, despite having only the fourth highest CDD value, Kolkata ranks second in its risk score in the 2.0°C warmer world due to its high population. Thus, population increase will primarily govern the risk associated with CDD in the 2.0°C warmer world. Notable exceptions are Bengaluru and Ahmedabad, higher CDD values make Ahmedabad at higher risk than Bengaluru despite a lower population.

The 3.0°C warmer world results in much more complex interactions between hazard, vulnerability and exposure metrics, neither attaining any statistically significant correlation with the risk score. The highest risk score for this warming level is attained by Chennai owing to its highest CDD value, fourth highest population, and lower per capita GDP. Kolkata attains the second highest risk score primarily owing to its high population despite moderate CDD values. Mumbai ranks fourth in CDD related risk in this warming level due to rapid economic growth improving per capita GDP. Ironically, Jaipur, an urban district in a hot desert, maintains the lowest risk score across all future time periods owing to its lower CDD (cold winters) and population, despite having lower per capita GDP.

We further contrast the risk scores considering two vulnerability metrics. The relative contribution of non-renewables to electricity supplied to Bengaluru, Chennai, Delhi, Jaipur and

Kolkata is 85.0%, 52.1%, 58.1%, 50.0%, and 92.1%, respectively. The resulting risk scores indicate a significant impact of choice of the vulnerability definitions on inferred risk values (Figure 6, Supplementary Tables S3-S5). For the year 2011, Kolkata attains the highest risk score considering the energy-source as a vulnerability indicator, while Chennai attains the highest risk score when per capita GDP is considered. This is due to the high dependence on non-renewables for electricity in case of Kolkata, and the lower per capita GDP for Chennai. Bengaluru and Jaipur attain the 4^{th} and 5^{th} rank in risk score using either vulnerability metrics. Despite a higher per capita GDP and lower CDD, Bengaluru has a higher risk score than Jaipur due to its higher population. Using source of energy as a vulnerability metric further increases the difference in the risk score between Bengaluru and Jaipur due to the former's greater dependence on non-renewables.

The influence of energy source on risk score is more prominent as the warming levels increase (Figure 6). Due to its high dependence on non-renewables, Kolkata's risk score is the greatest across all risk values, the highest score of 9.11 attained in the 3.0°C warming level when energy source is considered. On similar lines, Bengaluru attains the second highest risk score across all urban districts for each warming level when considering energy source as a vulnerability metric, but fourth highest when considering per capita GDP. Considering per capita GDP, Chennai attains the highest risk score for 1.5°C and 3.0°C warming levels, surpassed by Kolkata only in the 2.0°C warming world. This is due to the complex influence of population, CDD changes and per capita GDP on the risk scores. Similarly, Jaipur always attains the lowest risk scores due to lowest population and lowest dependence on non-renewables. The energy-source based risk scores consistently increase in magnitude with rising warming levels, while per-capita GDP based risk scores attain the highest value at the 2.0°C warming level, thereby reducing in the 3.0°C warming level. This is due to a sharp rise in per capita GDP in the 3.0°C warming world, which compensates for the influence of increasing population and CDD.

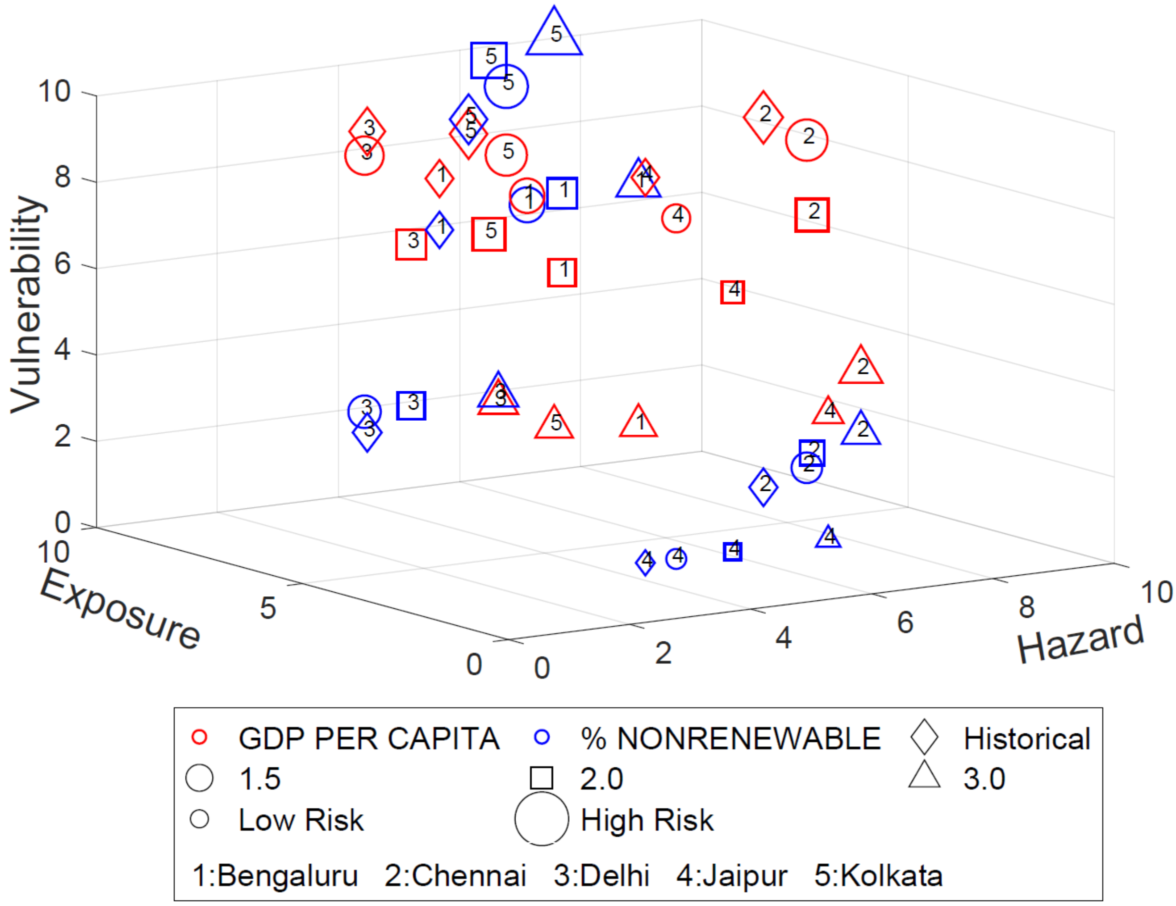

Figure 6. Vulnerability (z-axis), hazard (y-axis), and exposure (x-axis) for five urbanized districts of India in 2011 (historical), 1.5°C, 2.0°C and 3.0°C warming worlds. Size of markers represent the relative risk score. The marker type represents different time periods. Two colours differentiate vulnerability metrics based on per capita GDP (red) and percentage of non-renewable energy contribution to electricity (blue). Numbers corresponds to the urban districts. Note: axis values may be distorted due to viewing angles. Please refer to Supplementary Tables S3-S5 for details. GDP: Gross Domestic Product. (Coloured Figure)

4. Conclusions

Our results indicate a clear benefit of limiting global warming levels to below 1.5°C by limiting the rise in degree-days between 5-14% across majority of the country. Less than 10% of the administrative units across India are likely to experience average annual CDD exceeding 3690°C at the 1.5°C warming level. However, under the 3.0°C warming level, nearly 50% of the administrative units are likely to exceed this value. We identify Mumbai with highest risk score under 1.5°C and 2.0°C warming levels, and Chennai with the highest risk score in the 3.0°C warming level, when comparing the top ten urbanized regions using per capita GDP based vulnerability metric. Despite its higher average annual CDD values, Chennai remains second to Mumbai in two out of three warming levels due to the important role of population in determining risk scores.

Similarly, we find a considerable influence of the choice of vulnerability metric in determining the risk score. Kolkata consistently attains the highest risk score when energy-source is considered. On the other hand, Chennai is placed fourth out of five regions despite its higher CDD values due to its lower dependence on non-renewables. This also indicates the great role that energy policy will play in alleviating these risks. An increasing reliance on renewables is likely to offset the negative emission consequences of increasing CDDs. According to IEA (2021), India's long-term energy planning needs to account for potentially rising peak demands due to increase in air conditioning and other appliance use in households. It also needs to consider the need for increased flexibility in power systems to support renewable energy transition, including increase battery storage, coordinating use of electricity among domestic and agriculture sectors in a day, etc.

There are a number of ways our analysis can be improved to further strengthen its policy relevance. CDD is not a perfect indicator to measure cooling demands as it entirely driven by temperature. Additional variables such as humidity and solar radiation could provide detailed information on energy demands (Kumar et al. 2020; Maia-Silva et al. 2020; Rastogi et al. 2021). Future projections of humidity indicators at fine resolution would help the researchers to get the more robust findings. Our analysis also indicates a room for improvement in climate model reproduction of CDD values. Though climate models are generally to capture temperature quite well, our results point out the need to improve predictions in cold regions. Furthermore, due to unavailability of electricity source data at fine spatial resolution, our risk assessment is restricted to only five districts of India. To inform adaptation strategies across all India, there is a dire need of climatic, socio-economic, and energy data sets at fine spatial resolution.

India has come up with the India Action Cooling Plan in March 2019 to provide sustainable and smart cooling for the next 20 years (Cell,O., 2019) Although the plan seeks reduction in cooling demand and focuses on sustainable cooling to lower emissions, our analysis shows that the challenges will vary by cities. Rising temperatures, dense populations, and high-income levels will pose challenges to reduce the risk of CDDs in the urban cities of Kolkata, Chennai Delhi and Mumbai. With use of renewable energy sources and low GHG emission, efforts can be made in achieving sustainable cooling targets. India's target of 450 gigawatts renewable energy capacity by 2030 could be a stepping stone in the process of meeting India's sustainable goals (Gupta and Bonds 2020). Risk assessment presented here is first of its kind in analysing CDD risk by looking at existing vulnerabilities of most urban districts. Findings could also contribute to national level policies by highlighting the gravity of adapting renewable energy sources and motivating in achieving sustainable ways of fulfilling the cooling demand.

Declaration of competing interest: The authors declare that they have no known competing financial interests or personal relationships that could have appeared to influence the work reported in this paper.

Author's Contributions: A.Y. performed the formal analysis, contributed to the analysis of data, and writing of the paper. R.S. helped in numerical experiments, contributed to the writing, and supervised the work. R.K. helped in interpretation of the results, formulation of research goal and co-wrote the paper.

References

1. Ahmadalipour, A., Moradkhani, H. and Kumar, M., 2019. Mortality risk from heat stress expected to hit poorest nations the hardest. Climatic Change, 152(3), pp.569-579.
2. Antunes Azevedo J, Chapman L, Muller CL. 2015. Critique and suggested modifications of the degree-days methodology to enable long-term electricity consumption assessments: a case study in Birmingham, UK. Meteorol. Appl. 22(4): 789– 796
3. Ascione, F., Bianco, N., De Masi, R.F., Mauro, G.M. and Vanoli, G.P., 2017. Resilience of robust cost-optimal energy retrofit of buildings to global warming: A multi-stage, multi-objective approach. Energy and Buildings, 153, pp.150-167.
4. Badescu, V. and Zamfir, E., 1999. Degree-days, degree-hours and ambient temperature bin data from monthly-average temperatures (Romania). Energy conversion and management, 40(8), pp.885-900.

5. Balaban, O. and de Oliveira, J.A.P., 2017. Sustainable buildings for healthier cities: assessing the co-benefits of green buildings in Japan. Journal of cleaner production, 163, pp.S68-S78.
6. Basha, G., Kishore, P., Ratnam, M.V., Jayaraman, A., Kouchak, A.A., Ouarda, T.B. and Velicogna, I., 2017. Historical and Projected Surface Temperature over India during the 20 th and 21 st century. Scientific reports, 7(1), pp.1-10.
7. Bhatnagar, M., Mathur, J. and Garg, V., 2018. Determining base temperature for heating and cooling degree-days for India. Journal of Building Engineering, 18, pp.270-280.
8. Biardeau, L.T., Davis, L.W., Gertler, P. and Wolfram, C., 2020. Heat exposure and global air conditioning. Nature Sustainability, 3(1), pp.25-28.
9. Borah, P., Singh, M.K. and Mahapatra, S., 2015. Estimation of degree-days for different climatic zones of North-East India. Sustainable Cities and Society, 14, pp.70-81.
10. Bosello, F., Roson, R. and Tol, R.S., 2006. Economy-wide estimates of the implications of climate change: Human health. Ecological Economics, 58(3), pp.579-591.
11. Brager, G.S. and De Dear, R., 2001. Climate, comfort, & natural ventilation: a new adaptive comfort standard for ASHRAE standard 55.

12. Campbell, I., Kalanki, A. and Sachar, S., 2018. Solving the Global Cooling Challenge. The Rocky Mountain Institute, November.
13. Cançado, V., Brasil, L., Nascimento, N. and Guerra, A., 2008, August. Flood risk assessment in an urban area: Measuring hazard and vulnerability. In 11th International conference on urban drainage, Edinburgh, Scotland, UK (pp. 1-10).
14. Cardona, O.D., 2011. Disaster risk and vulnerability: Concepts and measurement of human and environmental insecurity. In Coping with global environmental change, disasters and security (pp. 107-121). Springer, Berlin, Heidelberg.
15. Cardoni, A., Noori, A.Z., Greco, R. and Cimellaro, G.P., 2021. Resilience assessment at the regional level using census data. International Journal of Disaster Risk Reduction, 55, p.102059.
16. Castañeda ME, Claus F. 2013. Variability and trends of heating degree-days in Argentina. Int. J. Climatol. 33(10): 2352– 2361.
17. Cell, O., 2019. India Cooling Action Plan. New Delhi: Ministry of Environment, Forest and Climate Change, Government of India. http://www. ozonecell. com/viewsection. jsp.
18. Christenson, M., Manz, H. and Gyalistras, D., 2006. Climate warming impact on degree-days and building energy demand in Switzerland. Energy conversion and management, 47(6), pp.671-686.

19. Ciancio, V., Salata, F., Falasca, S., Curci, G., Golasi, I. and de Wilde, P., 2020. Energy demands of buildings in the framework of climate change: An investigation across Europe. Sustainable Cities and Society, 60, p.102213.
20. Crichton, D., 1999. The risk triangle. Natural disaster management, 102(3).
21. De Rosa, M., Bianco, V., Scarpa, F. and Tagliafico, L.A., 2014. Heating and cooling building energy demand evaluation; a simplified model and a modified degree days approach. Applied energy, 128, pp.217-229.
22. Desai, A., Vaidya, P. and Pathella, S.,2019. A Simplified Method for Estimating Cooling Energy Savings Due to Passive Strategies for Indian Cities.
23. Dhorde, A.G. and Zarenistanak, M., 2013. Three-way approach to test data homogeneity: An analysis of temperature and precipitation series over southwestern Islamic Republic of Iran. J. Indian Geophys. Union, 17(3), pp.233-242.
24. Elizbarashvili, M., Chartolani, G. and Khardziani, T., 2018. Variations and trends of heating and cooling degree-days in Georgia for 1961–1990 year period. Annals of Agrarian Science, 16(2), pp.152-159.
25. Estoque, R.C., Ooba, M., Seposo, X.T., Togawa, T., Hijioka, Y., Takahashi, K. and Nakamura, S., 2020. Heat health risk assessment in Philippine cities using remotely sensed data and social-ecological indicators. Nature communications, 11(1), pp.1-12.

26. Frölicher, T.L., Fischer, E.M. and Gruber, N., 2018. Marine heatwaves under global warming. Nature, 560(7718), pp.360-364.
27. Gaffin, S.R., Rosenzweig, C., Xing, X. and Yetman, G., 2004. Downscaling and geo-spatial gridding of socio-economic projections from the IPCC Special Report on Emissions Scenarios (SRES). Global Environmental Change, 14(2), pp.105-123.
28. Gavrilov, M.B., Tošić, I., Marković, S.B., Unkašević, M. and Petrović, P., 2016. Analysis of annual and seasonal temperature trends using the Mann-Kendall test in Vojvodina, Serbia. Időjárás, 120(2), pp.183-198.
29. GRI, I.E. and GRI, E.I., 2018. Incorporating epidemics risk in the INFORM Global Risk Index.
30. Gupta, A.R. and Bonds, G., 2020. Financing India's renewable energy vision. Issue Brief, (336).
31. Gupta, E., 2012. Global warming and electricity demand in the rapidly growing city of Delhi: A semi-parametric variable coefficient approach. Energy economics, 34(5), pp.1407-1421.
32. Gupta, P., Verma, S., Bhatla, R., Chandel, A.S., Singh, J. and Payra, S., 2020. Validation of surface temperature derived from MERRA-2 Reanalysis against IMD gridded data set over India. Earth and Space Science, 7(1), p.e2019EA000910.
33. He, C., Ma, L., Zhou, L., Kan, H., Zhang, Y., Ma, W. and Chen, B., 2019. Exploring the mechanisms of heat wave vulnerability at the urban scale

based on the application of big data and artificial societies. Environment international, 127, pp.573-583.

34. Helsel, D.R. and Frans, L.M., 2006. Regional Kendall test for trend. Environmental science & technology, 40(13), pp.4066-4073.

35. Hoegh-Guldberg, O., Jacob, D., Bindi, M., Brown, S., Camilloni, I., Diedhiou, A., Djalante, R., Ebi, K., Engelbrecht, F., Guiot, J. and Hijioka, Y., 2018. Impacts of 1.5 C global warming on natural and human systems. Global warming of 1.5 C. An IPCC Special Report.

36. Hossain, M.U. and Poon, C.S., 2018. Global warming potential and energy consumption of temporary works in building construction: A case study in Hong Kong. Building and Environment, 142, pp.171-179. Baldwin, J.W., Dessy, J.B., Vecchi, G.A. and Oppenheimer, M., 2019. Temporally compound heat wave events and global warming: An emerging hazard. Earth's Future, 7(4), pp.411-427.

37. International Energy Agency, “India Energy Outlook 2021” (Paris: International Energy Agency, 2021) https://www.iea.org/reports/india-energy-outlook-2021.

38. IPCC (2014) Summary for policymakers In: Field CB et al (eds) Climate Change 2014: Impacts, Adaptation, and Vulnerability. Part A: Global and Sectoral Aspects. Contribution of Working Group II to the Fifth Assessment Report of the Intergovernmental Panel on Climate Change, Cambridge University Press, Cambridge, and New York, pp 1–32

39. Irannezhad, M., Marttila, H. and Kløve, B., 2014. Long-term variations and trends in precipitation in Finland. International Journal of Climatology, 34(10), pp.3139-3153.
40. Jagarnath, M., Thambiran, T. and Gebreslasie, M., 2020. Heat stress risk and vulnerability under climate change in Durban metropolitan, South Africa—identifying urban planning priorities for adaptation. Climatic Change, 163(2), pp.807-829.
41. Jaiswal, R.K., Lohani, A.K. and Tiwari, H.L., 2015. Statistical analysis for change detection and trend assessment in climatological parameters. Environmental Processes, 2(4), pp.729-749.
42. Kadioglu, M. and Şen, Z., 1999. Degree-day formulations and application in Turkey. Journal of Applied Meteorology, 38(6), pp.837-846.
43. Kazmierczak, A. and Cavan, G., 2011. Surface water flooding risk to urban communities: Analysis of vulnerability, hazard and exposure. Landscape and Urban Planning, 103(2), pp.185-197.
44. Kendall, M., 1975. Rank correlation measures. Charles Griffin, London, 202, 15.
45. Khosla, R., Agarwal, A., Sircar, N. and Chatterjee, D., 2021. The what, why, and how of changing cooling energy consumption in India's urban households. Environmental Research Letters, 16(4), p.044035.

46. Kumar, P. and Sarthi, P.P., 2019. Surface temperature evaluation and future projections over India using CMIP5 models. Pure and Applied Geophysics, 176(11), pp.5177-5201.
47. Kumar, R., Rachunok, B., Maia-Silva, D. and Nateghi, R., 2020. Asymmetrical response of California electricity demand to summer-time temperature variation. Scientific reports, 10(1), pp.1-9.
48. Kumar, Rohini, and Vimal Mishra. "Increase in population exposure due to dry and wet extremes in India under a warming climate." Earth's Future 8, no. 12 (2020): e2020EF001731.
49. Lee, K., Baek, H.J. and Cho, C., 2014. The estimation of base temperature for heating and cooling degree-days for South Korea. Journal of applied meteorology and climatology, 53(2), pp.300-309.
50. Lipson, M.J., Thatcher, M., Hart, M.A. and Pitman, A., 2019. Climate change impact on energy demand in building-urban-atmosphere simulations through the 21st century. Environmental Research Letters, 14(12), p.125014.
51. Liu, Z., Mehran, A., Phillips, T.J. and AghaKouchak, A., 2014. Seasonal and regional biases in CMIP5 precipitation simulations. Climate Research, 60(1), pp.35-50.
52. Lohmann, U., Stier, P., Hoose, C., Ferrachat, S., Kloster, S., Roeckner, E. and Zhang, J., 2007. Cloud microphysics and aerosol indirect effects in the

global climate model ECHAM5-HAM. Atmospheric Chemistry and Physics, 7(13), pp.3425-3446.

53. Maia-Silva, D., Kumar, R. and Nateghi, R., 2020. The critical role of humidity in modeling summer electricity demand across the United States. Nature communications, 11(1), pp.1-8.

54. Masson-Delmotte, V., Zhai, P., Pörtner, H.O., Roberts, D., Skea, J., Shukla, P.R., Pirani, A., Moufouma-Okia, W., Péan, C., Pidcock, R. and Connors, S., 2018. Global warming of 1.5 C. An IPCC Special Report on the impacts of global warming of, 1(5).

55. Mc Intyre GN, Kliewer WM, Lider LA. 1987. Some limitations of the degree day system as used in viticulture in California. Am. J. Enol. Vitic. 38(2): 128– 132.

56. Mishra, V., Tiwari, A.D., Aadhar, S., Shah, R., Xiao, M., Pai, D.S. and Lettenmaier, D., 2019. Drought and famine in India, 1870–2016. Geophysical Research Letters, 46(4), pp.2075-2083.

57. Morakinyo, T.E., Ren, C., Shi, Y., Lau, K.K.L., Tong, H.W., Choy, C.W. and Ng, E., 2019. Estimates of the impact of extreme heat events on cooling energy demand in Hong Kong. Renewable Energy, 142, pp.73-84.

58. Moral-Carcedo J, Vicens-Otero J. 2005. Modelling the non-linear response of Spanish electricity demand to temperature variations. Energy Econ. 27(3): 477– 494.

59. Ministry of Statistics and Programme Implementation Government of India (MoSPI) 2020, Energy Statistics 2020; https://www.niua.org/csc/assets/pdf/key-documents/phase-2/Energy-Green-Building/Energy-Statistics-2020.pdf
60. Murakami, D. and Yamagata, Y., 2019. Estimation of gridded population and GDP scenarios with spatially explicit statistical downscaling. Sustainability, 11(7), p.2106.
61. Nerini, F.F., Tomei, J., To, L.S., Bisaga, I., Parikh, P., Black, M., Borrion, A., Spataru, C., Broto, V.C., Anandarajah, G. and Milligan, B., 2018. Mapping synergies and trade-offs between energy and the Sustainable Development Goals. Nature Energy, 3(1), pp.10-15.
62. Olivier, J.G., Peters, J.A. and Janssens-Maenhout, G., 2013. Trends in global CO2 emissions. 2013 report. Available online at: https://www.pbl.nl/sites/default/files/downloads/pbl-2013-trends-in-global-co2-emissions-2013-report-1148_0.pdf
63. O'Neill, B.C., Kriegler, E., Riahi, K., Ebi, K.L., Hallegatte, S., Carter, T.R., Mathur, R. and van Vuuren, D.P., 2014. A new scenario framework for climate change research: the concept of shared socioeconomic pathways. Climatic change, 122(3), pp.387-400.
64. Petri, Y. and Caldeira, K., 2015. Impacts of global warming on residential heating and cooling degree-days in the United States. Scientific reports, 5(1), pp.1-14.

65. Pettitt, A.N., 1979. A non-parametric approach to the change-point problem. Journal of the Royal Statistical Society: Series C (Applied Statistics), 28(2), pp.126-135.
66. Philip, D. and Rayhan, M.I., 2004. Vulnerability and Poverty: What are the causes and how are they related. ZEF Bonn, center for Development Research, University of Bonn.
67. Prabnakorn, S., Maskey, S., Suryadi, F.X. and de Fraiture, C., 2019. Assessment of drought hazard, exposure, vulnerability, and risk for rice cultivation in the Mun River Basin in Thailand. Natural Hazards, 97(2), pp.891-911.
68. Quayle, R.G. and Diaz, H.F., 1980. Heating degree day data applied to residential heating energy consumption. Journal of Applied Meteorology and Climatology, 19(3), pp.241-246.
69. Ramon, D., Allacker, K., De Troyer, F., Wouters, H. and van Lipzig, N.P., 2020. Future heating and cooling degree days for Belgium under a high-end climate change scenario. Energy and Buildings, 216, p.109935.
70. Rastogi, D., Lehner, F., Kuruganti, T., Evans, K.J., Kurte, K.R., and Sanyal, J., 2021. The role of humidity in determining future electricity demand in the southeastern United States. Environmental Research Letters.
71. Reverter, M., Sarter, S., Caruso, D., Avarre, J.C., Combe, M., Pepey, E., Pouyaud, L., Vega-Heredía, S., De Verdal, H. and Gozlan, R.E., 2020.

Aquaculture at the crossroads of global warming and antimicrobial resistance. Nature communications, 11(1), pp.1-8.

72. Riahi, K., Van Vuuren, D.P., Kriegler, E., Edmonds, J., O’neill, B.C., Fujimori, S., Bauer, N., Calvin, K., Dellink, R., Fricko, O. and Lutz, W., 2017. The Shared Socioeconomic Pathways and their energy, land use, and greenhouse gas emissions implications: An overview. Global environmental change, 42, pp.153-168.

73. Sailor, D.J. and Muñoz, J.R., 1997. Sensitivity of electricity and natural gas consumption to climate in the USA—Methodology and results for eight states. Energy, 22(10), pp.987-998.

74. Sailor, D.J., 2011. A review of methods for estimating anthropogenic heat and moisture emissions in the urban environment. International journal of climatology, 31(2), pp.189-199.

75. Sedai, A.K., Nepal, R. and Jamasb, T., 2021. Flickering lifelines: Electrification and household welfare in India. Energy Economics, 94, p.104975.

76. Shanmugapriya, S., Premalatha, M., Rajkumar, S.R. and Thirunavukkarasu, I., 2011. Analysis of Colling Degree Days for Tiruchirappalli-A District In India. International Journal of Research and Reviews in Applied Sciences, 8(1), pp.44-56.

77. Shi, Y., Wang, G., Gao, X. and Xu, Y., 2018. Effects of climate and potential policy changes on heating degree days in current heating areas of China. Scientific reports, 8(1), pp.1-13.
78. Sieck, K., Nam, C., Bouwer, L.M., Rechid, D. and Jacob, D., 2021. Weather extremes over Europe under 1.5 and 2.0° C global warming from HAPPI regional climate ensemble simulations. Earth System Dynamics, 12(2), pp.457-468.
79. Singh, R. and Kumar, R., 2019. Climate versus demographic controls on water availability across India at 1.5 C, 2.0 C and 3.0 C global warming levels. Global and planetary change, 177, pp.1-9.
80. Sivak, M., 2008. Where to live in the United States: combined energy demand for heating and cooling in the 50 largest metropolitan areas. Cities, 25(6), pp.396-398.
81. Sneyers, R., 1991. On the statistical analysis of series of observations (No. 143).
82. Spinoni, J., Vogt, J.V., Barbosa, P., Dosio, A., McCormick, N., Bigano, A. and Füssel, H.M., 2018. Changes of heating and cooling degree-days in Europe from 1981 to 2100. International Journal of Climatology, 38, pp.e191-e208.
83. Thom, E.C., 1959. The discomfort index. Weatherwise, 12(2), pp.57-61.
84. Thom, H.C.S., 1952. Seasonal degree-day statistics for the United States. Monthly Weather Review, 80(9), pp.143-147.

85. Ukey, R. and Rai, A.C., 2021. Impact of Global Warming on Heating and Cooling Degree Days in Major Indian Cities. Energy and Buildings, p.111050.

86. UNFCCC. Intended National Determined Contributions (INDC) Submissions. United Nations Framework Convention on Climate Change, individual country's INDC can be found at the following website: https://www4.unfccc.int/Submissions/INDC/; 2015.

87. UNISDR. Words into Action Guidelines,2017. National Disaster Risk Assessment. Governance System, Methodologies, and Use of Results. (United Nations Office for Disaster Risk Reduction, Geneva, Switzerland.

88. Van Vuuren, D.P., Edmonds, J., Kainuma, M., Riahi, K., Thomson, A., Hibbard, K., Hurtt, G.C., Kram, T., Krey, V., Lamarque, J.F. and Masui, T., 2011. The representative concentration pathways: an overview. Climatic change, 109(1), pp.5-31.

89. Vautard, R., Gobiet, A., Sobolowski, S., Kjellström, E., Stegehuis, A., Watkiss, P., Mendlik, T., Landgren, O., Nikulin, G., Teichmann, C. and Jacob, D., 2014. The European climate under a 2° C global warming. Environmental Research Letters, 9(3), p.034006.

90. Verstraeten, G., Poesen, J., Demarée, G. and Salles, C., 2006. Long-term (105 years) variability in rain erosivity as derived from 10-min rainfall depth data for Ukkel (Brussels, Belgium): Implications for assessing soil erosion rates. Journal of Geophysical Research: Atmospheres, 111(D22).

91. Wang XM, Chen D, Ren ZG. 2010. Assessment of climate change impact on residential building heating and cooling energy requirement in Australia. Build. Environ. 45: 1663– 1682.
92. Warszawski, L., Frieler, K., Huber, V., Piontek, F., Serdeczny, O. and Schewe, J., 2014. The inter-sectoral impact model intercomparison project (ISI–MIP): project framework. Proceedings of the National Academy of Sciences, 111(9), pp.3228-3232.
93. Yaduvanshi, A., Bendapudi, R., Nkemelang, T. and New, M., 2021. Temperature and rainfall extremes change under current and future . global warming levels across Indian climate zones. Weather and Climate Extremes, 31, p.100291.
94. Yildiz, I. and Sosaoglu, B., 2007. Spatial distributions of heating, cooling, and industrial degree-days in Turkey. Theoretical and Applied Climatology, 90(3), pp.249-261
95. Zhang, C., Kazanci, O.B., Levinson, R., Heiselberg, P., Olesen, B.W., Chiesa, G., Sodagar, B., Ai, Z., Selkowitz, S., Zinzi, M. and Mahdavi, A., 2021. Resilient cooling strategies–A critical review and qualitative assessment. Energy and Buildings, 251, p.111312.
96. Zhang, W., Zhou, T., Zhang, L. and Zou, L., 2019. Future intensification of the water cycle with an enhanced annual cycle over global land monsoon regions. Journal of Climate, 32(17), pp.5437-5452.

97. Zhao, D., Aili, A., Yin, X., Tan, G. and Yang, R., 2019. Roof-integrated radiative air-cooling system to achieve cooler attic for building energy saving. Energy and Buildings, 203, p.109453.

98. Zhu, B., Su, B. and Li, Y., 2018. Input-output and structural decomposition analysis of India's carbon emissions and intensity, 2007/08–2013/14. Applied Energy, 230, pp.1545-1556.